PHYSICAL REVIEW B VOLUME 21, NUMBER 8 15 APRIL 1980

Wave-vector decomposition of the exchange and correlation contributions to a metallic surface energy

M. Rasolt
Solid State Division, Oak Ridge National Laboratory, Oak Ridge, Tennessee 37830

D. J. W. Geldart
Department of Physics, Dalhousie University, Halifax, Nova Scotia, Canada B3H 3J5
(Received 2 July 1979)

We decompose the lowest-order nonlocal corrections to the local-density approximation to the exchange and correlation component of the metallic surface energy in terms of its wave-vector components. Comparison with the full exchange shows significant improvement over the local-density form. An interpolation between the surface-plasmon-dominated small-wave-vector contributions and the nonlocal correction for large q is suggested, and some of the difficulties inherent in this method are discussed.

I. INTRODUCTION

In a recent paper[1] (to be referred to as I) Rasolt, Malmstrom, and Geldart have analyzed in great detail the implication of a procedure[2,3] which attempts to incorporate surface-plasmon contributions in the exchange and correlation energy (E_{xc}) of a metallic surface. This scheme [called the wave-vector interpolation (WVI)] which relies on being exact for both small and large wave-vector q fluctuations was shown (see I) to fail quantitatively in the intermediate-q range, precisely the range for which the WVI was designed.

An approximation for E_{xc} was suggested by Hohenberg and Kohn,[4] which is referred to as the local density approximation (LDA). In the LDA E_{xc} is approximated by

$$E_{xc} \approx E_{xc}^{LD} = \int d^3r\, n(\vec{r})\epsilon_{xc}(n(\vec{r})), \tag{1}$$

where $\epsilon_{xc}(n(\vec{r}))$ is the exchange-correlation energy per electron of a homogeneous electron gas of density $n(\vec{r})$. Equation (1) can be decomposed in terms of its wave-vector components[2,3] (see also I). Then

$$E_{xc}^{LD} = \tfrac{1}{2}\int \frac{d^3q}{(2\pi)^3}\int d^3r \int_0^1 d\lambda\, v(\vec{q})n(\vec{r}) \times[S_\lambda^h(\vec{q}, n(\vec{r})) - 1], \tag{2}$$

where $S_\lambda^h(\vec{q}, n(\vec{r}))$ is the structure factor of the uniform electron gas with local density $n(\vec{r})$ and the integral over λ is the usual coupling-constant integration.[5] We will, in this paper, be interested exclusively in the exchange-correlation contribution to the surface energy; i.e., the energy (per unit area) required to cleave this uniform electron gas. We therefore define this energy as[2]

$$\sigma_{xc} \equiv \frac{E_{xc}}{2A} = \int_0^\infty \frac{dq}{k_F}\gamma(q), \tag{3}$$

where A is the area of the cleaved surface.

Equation (1), or equivalently (2) is expected to be adequate for large q. For q in the intermediate- or small-wave-vector region Hohenberg and Kohn suggested a nonlocal correction E_{xc}^{nl} of the form:

$$E_{xc}^{nl} = -\tfrac{1}{4}\int d^3r \int d^3r'\, K_{xc}(\vec{r}-\vec{r}'; n(\vec{r}_0)) \times [(n(\vec{r}) - n(\vec{r}'))^2], \tag{4}$$

with K_{xc} related to the response function of the uniform electron gas.[4] Since both Eqs. (1) and (4) are related to the uniform system they are not at all likely to contain the contributions of surface plasmons, contributions which are related to the global surface geometry. Such terms which dominate $E_{xc}(\vec{q})$ for small wave-vector fluctuations[2,6,7] have, however, rigorous $q \to 0$ limit[2] given by

$$\sigma_{xc} = \int \frac{dq}{k_F}\gamma(q) = \int \frac{dq}{k_F}\left(\frac{k_F q}{8\pi}(\omega_s - \tfrac{1}{2}\omega_p)\right), \tag{5}$$

where

$$k_F = (3\pi^2 n_0)^{1/3}, \quad \omega_p = \left(\frac{4\pi e^2 n_0}{m}\right)^{1/2},$$

n_0 is the bulk density, and ω_s the surface-plasmon frequency $\omega_s = \omega_p/\sqrt{2}$. The WVI suggests a simple interpolation (see also I) between Eqs. (2) and (5) which turns out to be inadequate. In this paper we suggest one possible improvement by approximately including the contribution of Eq. (4) in the WVI.

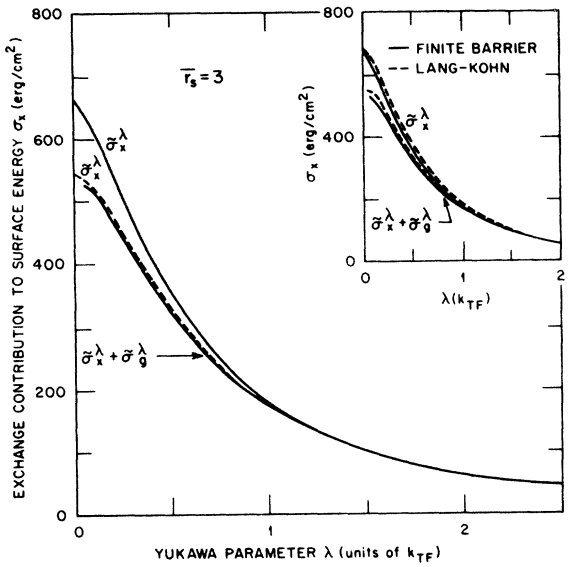

FIG. 1. Taken from Ref. 8. The dashed curve is the full HF surface energy for the finite-barrier model as a function of λ (see text). The barrier height is set equal to $\mu_0 = \hbar^2 k_F^2/2m$. The solid curves σ_x^λ and $\sigma_x + \sigma_g$ are the surface energies of the local density and local density with gradient corrections, respectively. The insert compares the local and gradient contributions calculated with model and Lang-Kohn[13] densities, and it is clear that this model represents the true density very well.

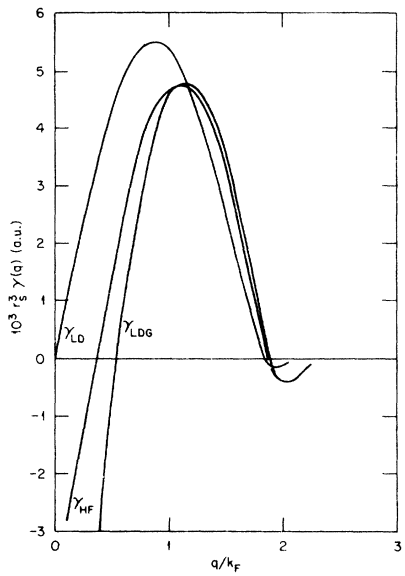

FIG. 2. Wave-vector decomposition of the exchange contribution to the surface energy of the IBM with bare Coulomb interparticle interaction. The curve labeled γ_{LD} is the LDA [Eq. (7)]; curve labeled γ_{LDG} is the LDA plus gradient [Eq. (22)], and the curve labeled γ_{HF} is the full exchange results. It should be pointed out that γ_{LDG} goes like $q^{-1/2}$ for small q in the IBM. This pathological behavior is an artifact of the IBM (see Sec. II) and does not occur for realistic density profiles.

An approximate treatment of Eq. (4) is to expand K_{xc} in a gradient expansion,[4] i.e.,

$$E_{xc}^{nl} \approx \int d^3r\, B_{xc}(n(\vec{r}))\nabla n(\vec{r})\cdot\nabla n(\vec{r}). \tag{6}$$

The convergence of such an expansion has been carefully examined in the case of a model Hartree-Fock surface-energy calculation[8] (see Fig. 1) with a *realistic* surface-density variation and found to be very adequate. We therefore suggest, as an improvement to WVI, not to interpolate between Eqs. (2) and (5) (Ref. 2) but rather to decompose the gradient contribution in Eq. (6) into its q-vector components[9] and treat both Eqs. (5) and (6) as corrections to LDA [Eqs. (1) or (2)] in the small- and large-q regions, respectively.

In Sec. II we present a detailed study of the q-vector decomposition of Eq. (6) for exchange contributions alone. In Sec. III we include the correlation contribution to Eq. (6). In Sec. IV we draw conclusions concerning some of the difficulties and many uncertainties inherent in this procedure.

The problem of presenting a unique and unambiguous structure for $E_{xc}(n(\vec{r}))$ at a metal surface, which includes surface-plasmon contributions, is a long standing and yet unsolved problem.[10,11] The purpose of the present work is to present some additional results which might motivate such a solution.

II. q-VECTOR DECOMPOSITION FOR THE EXCHANGE SURFACE ENERGY

In this section we study in considerable detail the WVI within the Hartree-Fock (HF) approximation alone. Such a detailed study within the LDA was presented in I and the results are repeated for completeness in Figs. 2 and 3. The curve labeled γ_{LD} is evaluated from Eq. (2) with S_λ^h the HF structure factor. In other words,

$$\gamma_{LD}(q) = \frac{v(q)q^2k_F}{4\pi^2}\int d^3r\, n(\vec{r})\left\{\theta(2k_F(\vec{r})-q)\left[-2+\frac{3}{2}\frac{q}{k_F(\vec{r})}-\frac{1}{8}\left(\frac{q}{k_F(\vec{r})}\right)^3\right]-\theta(2k_F-q)\left[-2+\frac{3}{2}\frac{q}{k_F}-\frac{1}{8}\left(\frac{q}{k_F}\right)^3\right]\right\}, \tag{7}$$

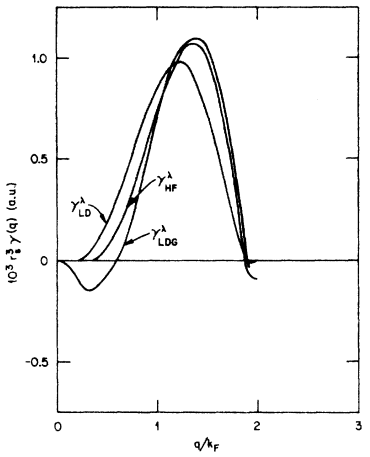

FIG. 3. Same as Fig. 2 but with a Yukawa interparticle interaction $4\pi e^2/(q^2+\lambda^2)$. The screening length λ is set equal to $2\lambda_{TF}$ and the density corresponds to $r_s=2$.

where $\theta^{>}(x)=1$ for $x>0$ and 0 for $x<0$ with $k_F(\vec{r})=[3\pi^2 n(\vec{r})]^{1/3}$. The metal surface considered was that of the infinite-barrier model (IBM), where

$$n(\vec{r})=n(z)=n_0\{1+(3/y^3)[y\cos(y)-\sin(y)]\} \tag{8}$$

with $y=2k_F z$ and z the axis perpendicular to the surface. This density was introduced in Eq. (7) and $v(\vec{q})$ was set equal to the bare Coulomb interaction $(4\pi e^2/q^2)$ in Fig. 2 and to $v(q)=4\pi e^2/(q^2+\lambda^2)$ in Fig. 3. The bulk density $n_0=1/[(4\pi/3)r_s^3]$ was set equal to $r_s=2$, and $\lambda=2\lambda_{FT}$ with $\lambda_{FT}=4k_F/\pi a_b$ and $a_b=\hbar^2/me^2$.

The full HF-IBM results (γ_{HF}) are also presented in Figs. 2 and 3 for the bare and Yukawa interactions. These results correspond to the surface-energy contribution from a single Fourier component q of the well-known form for the exchange energy, i.e.,

$$E_x=-\tfrac{1}{4}\int d^3r\int d^3r'\, v(\vec{q})e^{i\vec{q}\cdot(\vec{r}-\vec{r}')}|\rho(\vec{r},\vec{r}')|^2, \tag{9}$$

where $\rho(\vec{r},\vec{r}')$ is the second-order density matrix. The analyses of Eq. (9) leading to the results of Figs. 2 and 3 are covered in considerable detail in I.

Clearly, for the IBM, the LDA and the full HF show significant deviations, and as shown in I these differences cannot be accounted for by the WVI even when correlations are included. Of particular concern are the differences in the region of q around k_F (see I). Therefore, any correction to the WVI should be closely scrutinized and with this in mind we turn to the contribution of Eq. (6). Our task is to decompose Eq. (6) into its q-vector fluctuations within exchange alone; we reserve the calculation of correlation for the following section. The sum of $E_x^{nl}(q)$ and the LDA will then be compared with the full IBM-HF surface energy (Figs. 2 and 3).

Before we turn to the treatment of Eq. (6) we make a brief comment concerning the convergence of Eqs. (1) and (6). The IBM density when inserted in Eq. (6) results in a very poor convergence for the surface energy for a wide range of Yukawa screening lengths.[12] When the full HF surface-energy calculation was carried out for a *finite*-barrier model (in which a realistic density profile similar to that of Lang and Kohn[13] can be achieved[12]), the convergence was found to be very adequate (Fig. 1). It would therefore be preferable to examine $E_x^{nl}(\vec{q})$ within the finite-barrier model. Unfortunately, no wave-vector decomposition has been carried out for such a model. Nevertheless, some interesting conclusions can still be drawn from the decomposition of Eq. (6) within the IBM (see below).

The coefficient B_{xc} in Eq. (6) is related to the response function $F(\vec{k})$ (Ref. 14) through

$$B_{xc}=\tfrac{1}{2}(a^2b-a_0^2b_0) \tag{10}$$

and

$$F(\vec{k})=a^{-1}+bk^2+O(k^4), \tag{11}$$

where a_0 and b_0 refer to the $\vec{k}$ expansion of the static Lindhard screening function and $a=-d\mu/dn$, where μ denotes the exact chemical potential [we use here for $F(\vec{k})$ the convention of Ref. 14]. The *full* exchange form of the undecomposed B_x has been derived by Geldart and Rasolt[15] (to be referred to as II) for the ladder graphs in Fig. 1 of II. To decompose it in terms of *individual* q-vector fluctuations immediately presents a considerable task for a number of reasons. We will therefore restrict our analysis in this work to the lowest-order exchange [Fig. 3(a) of II] and correlation [Figs. 3(b) and 3(c) of II] graphs. (We return to this point in Sec. IV.)

Following standard analysis[16] the contribution to a^{-1} from the terms in Fig. 3 of II is written

$$a^{-1}=a_0^{-1}+2\,\mathrm{tr}_p\frac{\partial}{\partial\mu_0}\left(\Sigma(p)\frac{\partial}{\partial\mu_0}G_0(p)\right)$$
$$-\frac{m}{\pi^2k_F}\Sigma(k_F,0), \tag{12}$$

with a_0^{-1} the Lindhard contribution given by $a_0^{-1}=-mk_F/\pi^2$, $\mu_0=k_F^2/2m$, and for notational convenience we set $\hbar=1$. The contributions to b are given in II and are summarized

$$b = b_0 + b' + b'' + b''' - \frac{m^2}{12\pi^2 k_F^3}\Sigma(k_F, 0) \tag{13}$$

with b_0 the Lindhard contribution given by $b_0 = m/12\pi^2 k_F$, and where

$$b' = -\frac{1}{m}\mathrm{tr}_p \frac{\partial}{\partial \mu_0}\left[\Sigma(p)\left(\frac{1}{2}\frac{\partial^2}{\partial \mu_0^2}G_0(p) - \frac{1}{9}\epsilon_{\vec{p}}\frac{\partial^3}{\partial \mu_0^3}G_0(p)\right)\right], \tag{14}$$

$$b'' = \frac{1}{m}\frac{1}{6}\mathrm{tr}_p\left(\Sigma(p)\frac{\partial^3}{\partial \mu_0^3}G_0(p)\right), \tag{15}$$

and

$$b''' = -\tfrac{1}{24}\mathrm{tr}_q\{[\partial F_0(q)/\partial \mu_0]^2[V(q)\nabla_{\vec{q}}^2 V(q) - |\nabla_{\vec{q}} V(q)|^2]\}. \tag{16}$$

In Eqs. (12)–(15) p is a four energy-momentum vector $p \equiv (p, p_0)$, $\epsilon_{\vec{p}} = p^2/m$, $G_0(p)$ is the single-particle propagator given by

$$G_0(p) = \frac{1}{p_0 - \epsilon_{\vec{p}} + \mu_0 + i\delta\,\mathrm{sgn}(\epsilon_{\vec{p}} - \mu_0)}, \tag{17}$$

and $\Sigma(p)$ the self-energy given by

$$\Sigma(p) = -\mathrm{tr}_q[V(q)G_0(p+q)]. \tag{18}$$

The q in tr_q, $V(q)$, and $F_0(q)$ is a four vector $q \equiv (q, q_0)$ and $V(q) = v(\vec{q})$ in the HF, and $V(q) = v(\vec{q})[1/\epsilon(q) - 1]$ for correlation (see Sec. III). Finally $F_0(q)$ is the dynamic Lindhard screening function[14,15] related to $\epsilon(q)$ by $\epsilon(q) = 1 - 4\pi e^2/q^2 F_0(q)$ and

$$\mathrm{tr}_p(\cdots) \equiv \int \frac{d^4p}{(2\pi)^4 i}(\cdots). \tag{19}$$

Restricting the analysis of Eqs. (12)–(16) to the HF approximation, only b' and b'' contribute to b_x and the decomposed form for $(a_0 + a_x)^{-1}$ and b_x can be evaluated to yield

$$(a_0 + a_x)^{-1} = a_0^{-1} - \int \frac{d^3q}{(2\pi)^3} v(\vec{q}) \frac{m^2 q}{4\pi^2 k_F^2}\theta^>(2k_F - q) \tag{20}$$

and

$$b_x = b_0 + \frac{m^2}{24\pi^2 k_F^3}\int \frac{d^3q}{(2\pi)^3} v(\vec{q})\left(-\frac{q}{2k_F}\theta^>(2k_F - q) + \tfrac{11}{6}k_F\delta(q - 2k_F) + \frac{k_F^2}{3}\delta'(q - 2k_F)\right). \tag{21}$$

Combining Eqs. (3), (6), (10), (20), and (21) we get the following form for the gradient contribution to $\gamma(q)$ in the HF approximation:

$$\gamma_G(q) = \tfrac{1}{96}k_F q^2 v(\vec{q})\int dz\, \frac{|\nabla n(\vec{r})|^2}{k_F^6(\vec{r})}\left[-\tfrac{3}{2}q\theta^>(2k_F(\vec{r}) - q) + \tfrac{11}{6}k_F^2(\vec{r})\delta(q - 2k_F(\vec{r})) + \tfrac{1}{3}k_F^3(\vec{r})\delta'(q - 2k_F(\vec{r}))\right]. \tag{22}$$

It is this term we evaluate next for a range of q for two densities and two different interparticle interactions [$v(\vec{q})$]. We then combine it with the local-density term (Eq. 7) and compare the result with the full HF expression.

The first density we consider is the IBM density Eq. (8). Inserting it into Eq. (22) and integrating over z for two different $v(\vec{q})$ and combining it with Eq. (7), we get the results displayed in Figs. 2 and 3 by the curve labeled γ_{LDG}. Clearly the addition of γ_G does not bring the exact HF and γ_{LDG} to full agreement for bare or Yukawa $v(\vec{q})$. Nevertheless, it is also clear that the addition of γ_G brings γ_{LDG} and γ_{HF} to closer agreement (especially in the range of q around k_F). Since the WVI is designed to correct primarily for the region of $q < k_F$ this is an important change. While the interpolation from $\gamma_{\mathrm{LD}}(q)$ to the small-q region suggested by the WVI is invalid, the interpolation from γ_{LDG} could be a considerable improvement, particularly for a realistic density; we return to this point shortly.

In Fig. 3, λ was set equal to $2\lambda_{\mathrm{TF}}$. The motivation is that for large λ the full IBM HF and the LDA and the LDA plus gradient all agree closely.[12] Figure 3 demonstrates that close agreement between the total surface energy does not imply similar agreement between individual q vectors.

The excellent convergence for the finite-barrier density[8] (Fig. 1) strongly suggests that the agreement between γ_{LDG} and γ_{HF} (Figs. 2 and 3) is likely to improve further for realistic density variation. Unfortunately, no exact decomposition of γ_{HF} for a finite-barrier model exists to enable such a comparison (see Sec. IV). To get a feeling for the effect of a realistic density on γ_G we evaluate Eq. (22) with a model density profile of the form

$$n(z) = n_0/(1 + e^{-\beta y}) \tag{23}$$

with $y = 2k_F z$ and $\beta = 0.5$ adjusted to fit the aluminum density variation.[13] The results are presented in Fig. 4 for $\lambda = 0$ and $\lambda = 2\lambda_{\mathrm{TF}}$. The most striking feature is that the exaggerated behavior of γ_G at small q (Figs. 2 and 3) is strongly damped. Cou-

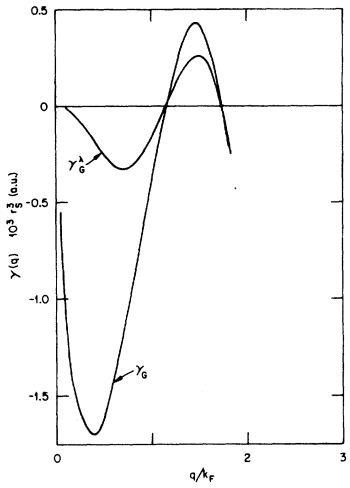

FIG. 4. Wave-vector decomposition of the gradient contributions alone [Eq. (22)] for a realistic density profile [Eq. (23)]. The curves labeled γ_G and γ_G^λ are for a bare Coulomb and a Yukawa interparticle interaction (with $\lambda = 2\lambda_{TF}$), respectively.

pled with the excellent overall agreement observed in Fig. 1 this leads us to conclude that the agreement between γ_{LDG} and γ_{HF} for real surface density[13] is likely to improve significantly.

In the following section we include the effect of correlation in γ_G and introduce the effect of surface-plasmon fluctuations at small q. In Sec. IV we return to the results presented above and draw some additional conclusions concerning the treatment of metallic surface energies.

III. q-VECTOR DECOMPOSITION FOR THE CORRELATION PART OF THE SURFACE ENERGY

The lowest-order contributions to the correlation part of a^{-1} and b are given also by Eqs. (12)–(16), the only change being that the static interparticle interaction now is replaced by $V(q) = v(\vec{q})[1/\epsilon(q) - 1]$. In addition the contribution of b''' (Eq. 16) is now present. This change of course greatly complicates the calculation, but fortunately most of the terms have been presented elsewhere (see II). We will therefore present only the final results below. For the term b' where the analysis deviates substantially from any previous calculations (see below) we will detail the key points of the derivation.

The calculation of the correlation contribution to a^{-1} is straightforward,[15] and the final form is given as

$$(a_0 + a_x + a_c)^{-1} - (a_0 + a_x)^{-1} \approx -a_c/a_0^2 = -e^4 m^3 y_c/(2\pi)^3 k_F^2 , \tag{24}$$

where

$$y_c = \frac{1}{\pi^2}\int_0^\infty dq \int_0^\infty dy \left[-\frac{Q(s,y)g(s,y)}{\tilde{\epsilon}(s,y)} + 2s\left(\frac{g(s,y)}{\tilde{\epsilon}(s,y)}\right)^2 + \frac{2Q(s,y)}{\tilde{\epsilon}(s,y)}\left(\frac{(1+s)}{(1+s)^2+y^2} - \frac{(1-s)}{(1-s)^2+y^2}\right)\right], \tag{25}$$

where

$$Q(s,y) = 2 + \frac{(y^2+1-s^2)}{2s} g(s,y) - 2y\left[\tan^{-1}\left(\frac{1+s}{y}\right) + \tan^{-1}\left(\frac{1-s}{y}\right)\right], \tag{26}$$

$$g(s,y) = \ln\left[\frac{y^2+(1+s)^2}{y^2+(1-s)^2}\right], \tag{27}$$

$$\tilde{\epsilon}(s,y) = s^2 + \frac{\alpha r_s}{4\pi} Q(s,y), \tag{28}$$

$s \equiv q/2k_F$, and $k_F a_b = 1/\alpha r_s$.

We next turn to the correlation contribution of Eqs. (13)–(16), to b, which is the most difficult part of the analysis. We begin with the last term of Eq. (13) which has been widely treated before,[17] and we write the final answer

$$\frac{-m^2}{12\pi^2 k_F^3}\Sigma(k_F,0) = \frac{m^3 e^4}{(2\pi)^3 k_F^4} Z_c^\mu , \tag{29}$$

where

$$Z_c^\mu = \frac{1}{12\pi^2}\int_0^\infty dq \int_0^\infty dy \frac{Q(s,y)g(s,y)}{\tilde{\epsilon}(s,y)} . \tag{30}$$

The contributions from b'' and b''' in Eqs. (15) and (16) were first evaluated in II, and we only list the final results. We write

$$b_c'' = \frac{e^4 m^3}{(2\pi)^3 k_F^4}(Z_c'' + Z_\delta'') . \tag{31}$$

The term Z_δ'' represents delta-function contributions [see Eq. (C16) of II] before their integration over q [the integration over q yields the last term in Eq. (60) of II]. It is

$$Z_\delta'' = \frac{-\pi}{6m}\int dq \frac{F(\vec{q},0)}{\epsilon(\vec{q},0)}\delta(k_F - \tfrac{1}{2}q) \tag{32}$$

with $F(\vec{q},0)$ the static Lindhard screening function and $\epsilon(\vec{q},0) = 1 - (4\pi e^2/q^2)F(\vec{q},0)$. Z_c'' is given by the first term of Eq. (60) of II and is

$$Z_c'' = \tfrac{4}{3}\int_0^\infty dq \int_0^\infty dy\, s \frac{Q(s,y)}{\tilde{\epsilon}(s,y)} H_2(s,y) , \tag{33}$$

where

$$H_2(s,y)=\frac{1}{8\pi^2 s^2}\left[\frac{(3+2s^2)(-y^2+s^2-1)+4s^2y^2}{(y^2+1-s^2)^2+4y^2s^2}\right.$$
$$\left.+\frac{(3-4s^2)[(y^2+1-s^2)^2-4s^2y^2]+16y^2(y^2+1-s^2)(\frac{3}{4}+s^2)}{[(y^2+1-s^2)^2-4y^2s^2]^2+16^2y^2(y^2+1-s^2)^2}\right]. \tag{34}$$

b''' is given in Eq. (61) of II (where a typographical error was made in the overall sign of b''') and is written below as

$$b_c'''=\frac{e^4m^3}{(2\pi)^3k_F^4}Z_c''' \tag{35}$$

with

$$Z_c'''=-\frac{1}{24\pi^2}\int_0^\infty dq\int_0^\infty\frac{dy}{s}\left(\frac{g(s,y)}{\tilde\epsilon(s,y)}\right)^2\left\{-1+\frac{\alpha r_s}{2\pi\tilde\epsilon(s,y)}\left[4-\tfrac{3}{2}Q(s,y)+\frac{(s^2+y^2)(3y^2-s^2+1)}{(y^2-s^2+1)^2+4y^2s^2}\right.\right.$$
$$\left.+\left(s-\frac{7}{4}\frac{(s^2+y^2)}{s}\right)g(s,y)\right]$$
$$+\frac{(\alpha r_s)^2}{8\pi^2(\tilde\epsilon(s,y))^2}\left[4+Q(s,y)\left(\tfrac{9}{4}Q(s,y)-6+\frac{3}{2}\frac{(s^2+y^2)}{s}g(s,y)\right)\right.$$
$$\left.\left.+g(s,y)\left(\frac{(s^2+y^2)^2}{4s^2}g(s,y)-\frac{2(s^2+y^2)}{s}\right)\right]\right\}. \tag{36}$$

The b' term of Eq. (14) is by far the most difficult contribution of b to calculate. The results presented in Eq. (59) of II unfortunately cannot be used for the decomposed structure of b. The reason is that to simplify the evaluation of b' the differentiation with respect to μ_0 was taken outside the tr_p. A careful inspection of Eq. (59) will convince the reader that the results no longer correspond to the proper q-vector decomposition. To properly decompose b' the direct differentiation of b' with the respect to μ_0 must be performed inside the integral to yield

$$b'=-\frac{1}{m}\mathrm{tr}_q v(\vec q)\frac{\partial\epsilon(q)}{\partial\mu_0}\frac{1}{[\epsilon(q)]^2}[\tfrac{1}{2}I_1(q)-\tfrac{1}{9}I_3(q)]+\frac{1}{m}\mathrm{tr}_q v(\vec q)\left(\frac{1}{\epsilon(q)}-1\right)\left(\frac{1}{2}\frac{\partial}{\partial\mu_0}I_1(q)-\frac{1}{9}\frac{\partial}{\partial\mu_0}I_3(q)\right); \tag{37}$$

the functions $I_1(q)$, $I_2(q)$, and $I_3(q)$ are the same as used in II. The additional difficulty arises from the last term in Eq. (37) which contains yet one higher derivative of $I_1(q)$ and $I_3(q)$ with respect to μ_0. The calculation is very lengthy. Particular attention should be paid to the higher-order delta-function contributions originating in $(\partial/\partial\mu_0)I_1(q)$ and $(\partial/\partial\mu_0)I_3(q)$. We present only the final results, writing

$$b'=\frac{m^3e^4}{(2\pi)^3k_F^4}(Z_c'+Z_\delta'); \tag{38}$$

then,

$$Z_\delta'=\int_0^\infty dq\left(-\frac{2\pi}{9m^2}\frac{k_F^4}{q^2}\frac{\partial F(\vec q,0)/\partial\mu_0}{[\epsilon(\vec q,0)]^2}\delta(k_F-\tfrac{1}{2}q)+\frac{4\pi}{9m}\frac{k_F^2}{q^2}\frac{F(\vec q,0)}{\epsilon(\vec q,0)}[7\delta(k_F-\tfrac{1}{2}q)-\tfrac{1}{2}k_F\delta'(k_F-\tfrac{1}{2}q)]\right) \tag{39}$$

and

$$Z_c'=-8\int_0^\infty dq\int_0^\infty dy\,s^2\left\{\frac{g(s,y)}{[\tilde\epsilon(s,y)]^2}[\tfrac{1}{2}H_1(s,y)-\tfrac{1}{9}H_3(s,y)]+\frac{sQ(s,y)}{\tilde\epsilon(s,y)}[\tfrac{1}{2}H_1'(s,y)-\tfrac{1}{9}H_3'(s,y)]\right\}, \tag{40}$$

where in Eq. (40)

$$H_1(s,y)=\frac{1}{8\pi^2s^2}\left(\frac{(1-2s^2)(-y^2+s^2-1)-2y^2(2s^2+1)}{(y^2+1-s^2)^2+4y^2s^2}+\frac{1}{4}\frac{1}{s}g(s,y)\right) \tag{41}$$

and

$$H_3(s,y)=\frac{1}{4\pi^2 s^2}\left(\frac{(\frac{3}{4}-2s^2)(-y^2+s^2-1)-2y^2(\frac{5}{4}+2s^2)}{(y^2+1-s^2)^2+4y^2s^2}\right.$$
$$\left.+y^2\frac{[4y^2s^2-(y^2+1-s^2)^2+2(y^2+1-s^2)(y^2-s^2)]}{[(y^2+1-s^2)^2-4y^2s^2]^2+16y^2s^2(y^2+1-s^2)^2}+\frac{3}{16}\frac{1}{s}g(s,y)\right)+\tfrac{1}{2}H_2(s,y)\,, \tag{42}$$

$$H_1'(s,y)=\frac{1}{4\pi^2 s^2}\left(\frac{(s^2-y^2-1)+s^2(y^2+s^2-1)}{[y^2+(s+1)^2][y^2+(s-1)^2]}\right.$$
$$\left.+\frac{2y^4-12y^2s^2+2s^4+4y^2-4s^2+2+(2s^2+1)[(y^2+s^2)(3y^2-s^2)+2(y^2+s^2)-1]}{[y^2+(s+1)^2]^2[y^2+(s-1)^2]^2}\right). \tag{43}$$

Finally

$$H_3'(s,y)=H_2(s,y)+H_3(s,y)+H_4(s,y)+H_5(s,y)\,, \tag{44}$$

where

$$H_4(s,y)=\frac{1}{4\pi^2 s^2}\left(\frac{\frac{3}{2}(y^2-s^2+1)+2s^2(-s^2-y^2+1)}{[y^2+(s+1)^2][y^2+(s-1)^2]}\right.$$
$$+\frac{\frac{3}{2}[y^4-6y^2s^2+s^4+2(y^2-s^2)+1]-3s^2[(y^2+s^2)(3y^2-s^2)+2(y^2+s^2)-1]}{[y^2+(s+1)^2]^2[y^2+(s-1)^2]^2}$$
$$+\frac{3[-7y^6+35y^4s^2-21y^2s^4+s^6-3(5y^4-10y^2s^2+s^4)+3(-3y^2+s^2)-1]}{[y^2+(s+1)^2]^3[y^2+(s-1)^2]^3}$$
$$\left.+\frac{4s^2[-(y^2+s^2)(5y^4-10y^2s^2+s^4)+3(y^2+s^2)(-3y^2+s^2)-3(y^2+s^2)+1]}{[y^2+(s+1)^2]^3[y^2+(s-1)^2]^3}\right)\,, \tag{45}$$

$$H_5(s,y)=\frac{1}{4\pi^2 s^2}\left(\frac{(4s^2+\frac{3}{4})(s^2+y^2-1)}{[y^2+(s+1)^2][y^2+(s-1)^2]}\right.$$
$$+\frac{4(y^4-y^2s^2+y^2)+3[y^4-6y^2s^2+s^4+2(y^2-s^2)+1]}{[y^2+(s+1)^2]^2[y^2+(s-1)^2]^2}$$
$$+\frac{\frac{1}{2}(8s^2+3)[-(y^2+s^2)(-3y^2+s^2)+2(y^2+s^2)-1]}{[y^2+(s+1)^2]^2[y^2+(s-1)^2]^2}$$
$$\left.-\frac{2[4y^2(y^2+s^2)^2(-s^2+y^2)+6(y^2+s^2)^2y^2-2y^2]}{[y^2+(s+1)^2]^3[y^2+(s-1)^2]^3}-\frac{3}{16}\frac{1}{s}g(s,y)\right). \tag{46}$$

This completes the first wave-vector decomposition of the correlation contribution to b. Combining Eqs. (29), (31), (35), and (38) we write

$$b_c=\frac{m^3e^4}{(2\pi)^3\hbar^4k_F}(Z_c+Z_\delta)\,, \tag{47}$$

where $Z_c=Z_c'+Z_c''+Z_c'''+Z_c^{\mu}$ and $Z_\delta=Z_\delta'+Z_\delta''$. To write the final form of the correlation contribution to $\gamma_G(q)$ we combine Eqs. (10), (24), and (47) to give

$$B_c=\int dq\,B_c(q,r_s)=\tfrac{1}{2}[a_0^2b_c+2b_0a_0a_c]$$
$$=\frac{e^2}{n^{4/3}}\left(\beta\frac{\alpha r_s}{k_F}(Z_c-\tfrac{1}{6}y_c)\right)+\frac{e^2}{n^{4/3}}\left(\beta\frac{\alpha r_s}{k_F}Z_\delta\right) \tag{48}$$

with $\beta=\pi/[16(3\pi^2)^{4/3}]$. The last term in Eq. (48) is the delta-function contribution to the q-vector decomposition of $B_c(q)$. To evaluate the first term of Eq. (48) for a fine mesh of q and r_s is simple since the integrals over y in Eqs. (25), (30), (33), (36), and (40) are straightforward except for a point singularity at $s=1$ of zero measure (a discontinuity). The contribution from correlation to $\gamma_G(q)$ is now given by[18]

$$\gamma_G(q)=k_F\int dz\,B_c(q,r_s(\vec{r}))\,|\nabla n(\vec{r})|^2\,. \tag{49}$$

The k_F multiplying the integral in Eq. (49) is the *bulk* Fermi momentum. For all the other k_F or r_s [including $s=q/2k_F(\vec{r})$ in Eqs. (24)–(27)] the *local* value of k_F at $\vec{r}$ given by $k_F(\vec{r})=[3\pi^2n(\vec{r})]^{1/3}$ must be used. In Figs. 5 and 6, Eq. (49) is evaluated for the IBM density (Eq. 8) and the more realistic density [Eq. (23)]. In the small-q range

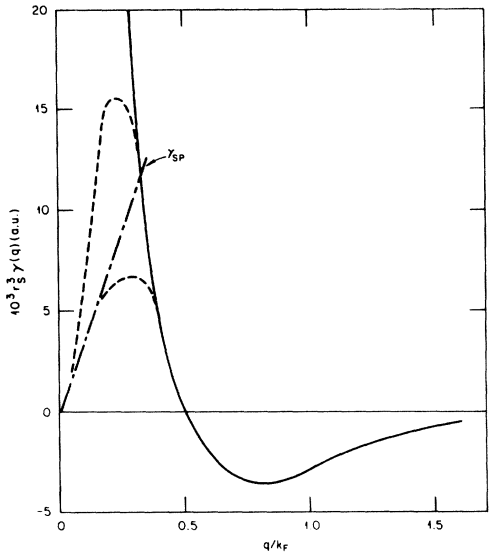

FIG. 5. Wave-vector decomposition for the sum of exchange and correlation gradient contributions [Eqs. (22) and (49)] within the IBM. The dash-dot line is the surface-plasmon contribution [Eq. (5)] and the two dashed curves indicate two possible interpolations between large- and small-q regions.

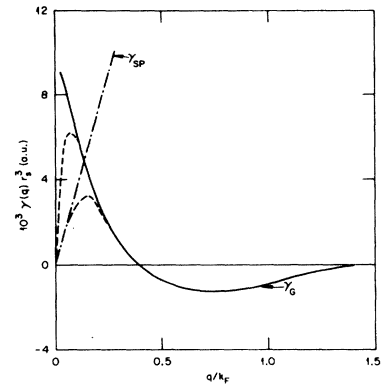

FIG. 6. Same as Fig. 5 but for the model density of Eq. (23).

the surface-plasmon contribution [Eq. (5)] is presented by the dash-dot line. Since $\gamma(q)$ is a continuous function of q the small- and large-q regions of Eqs. (5) and (6) must join smoothly. Two such possible interpolations are presented by the dashed curves in Figs. 5 and 6. In the following section we discuss some of the implications of the above results.

IV. CONCLUSIONS

In Secs. II and III we have shown how to decompose the nonlocal correction [$E_{xc}^{nl}(q)$, Eq. (4)] to the LDA in terms of its q-vector fluctuations. For large q the gradient expansion [Eq. (6)] was suggested as an approximation for $E_{xc}^{nl}(q)$. For small q, the surface-plasmon-dominated form[2,6,7] [Eq. (5)] was used to approximate Eq. (4). Since $\gamma(q)$ is a continuous function of q an interpolation between the two regions is suggested (Figs. 5 and 6). It is the arbitrary nature of this interpolation that is the core of the uncertainty inherent in this procedure; we return to this shortly.

If this procedure is to produce any confidence then it must be carefully examined in models where the result is known. It is particularly important that above the point q, from which we start the interpolation toward small q (Figs. 5 and 6), the accuracy of the decomposed gradient expansion is properly assessed. In Sec. II we examined this question within the HF alone for the IBM (Figs. 2 and 3). Although we discover a significant improvement over the LDA, major deviations do remain. These differences we argue will be further reduced in the case of a realistic density profile but a final conclusion must await a similar analysis within the finite-barrier model. To argue that correlation will correct these deviations is unfounded as the results in Figs. 2 and 3 (see also I) clearly demonstrate. Finally, we note that to include exchange and correlation contributions beyond the lowest-order corrections considered here this method presents further problems which must be overcome.

The interpolation between the surface plasmons and the gradient contributions is the most serious shortcoming of this scheme since the interpolation must be very sensitive to the density profile. To see this, consider a problem having a bulk-density variation, modeled to be very similar to the surface-density profile. The exact $\gamma(q)$ for the bulk problem, however, will deviate in a major way at small q from the $\gamma(q)$ of the surface problem, since for a bulk density no surface plasmons exist. Consequently, the two arbitrary interpolations suggested in Figs. 5 and 6 might be totally wrong and the correct small-q surface-plasmon behavior might be to vary rapidly and join $\gamma_G(q)$ at very small q in Fig. 6. In addition note the fact that the high-density limit (where local rather than global effects become important) of $\gamma_G(q)$ is dominated by the small-q region and is not going to be reproduced properly by naive treatments. The correct resolution of these very serious problems may well have to await a wave-vector decomposition of the exact exchange and correlation within the IBM and more realistic models. Finally we note that the developments presented in Secs. II and III are not restricted to surface studies alone and could

present some additional insight to the treatment of E_{xc} for bulk systems as well in which inhomogeneities such as impurity centers (for example) play a role.

In principle the structure of Eq. (4) can accomodate surface-plasmons contributions with appropriate extensions. The difficulty lies in discovering the structure of such a *universal* functional that contains and clearly exhibits these contributions. A key feature of such a functional must be its ability to discern the distinction between surface- and bulk-density profiles. The possibility of constructing such a universal functional through model calculations is currently being investigated.

ACKNOWLEDGMENTS

We wish to acknowledge Dr. J. Harris for critical reading of this manuscript. This research was partially supported by the Division of Materials Sciences, U. S. Department of Energy under Contract No. W-7405-eng-26 with the Union Carbide Corporation, and the National Research Council of Canada.

[1]M. Rasolt, G. Malmstrom, and D. J. W. Geldart, Phys. Rev. B 20, 3012 (1979).
[2]D. C. Langreth and J. P. Perdew, Phys. Rev. B 15, 2884 (1977) and Solid State Commun. 17, 1425 (1975).
[3]J. P. Perdew, D. C. Langreth, and V. Sahmi, Phys. Rev. Lett. 38, 1030 (1977).
[4]P. Hohenberg and W. Kohn, Phys. Rev. B 136, 864 (1964).
[5]D. Pines and P. Nozières, *Theory of Quantum Liquids* (Benjamin, New York, 1966).
[6]R. A. Craig, Phys. Rev. B 6, 1134 (1972).
[7]J. Schmit and A. A. Lucas, Solid State Commun. 11, 415 (1972).
[8]M. Rasolt, J. S. Y. Wang, and L. M. Kahn, Phys. Rev. B 15, 580 (1977).
[9]The first to decompose the gradient contribution in the high-density limit was V. Peuckert, J. Phys. C 9, 4173 (1976). Additional comments concerning this decomposition were made by M. Rasolt, G. Malmstrom, and D. J. W. Geldart at the APS meeting, 1979 in Chicago and by D. C. Langreth and J. P. Perdew at the APS meeting, 1979 in Chicago.
[10]J. C. Phillips, Comments Solid State Phys. 6, 91 (1975).
[11]W. Kohn and N. D. Lang, Comments Solid State Phys. 6, 95 (1975).
[12]J. S. Y. Wang and M. Rasolt, Phys. Rev. B 13, 5330 (1976).
[13]N. D. Lang and W. Kohn, Phys. Rev. B 1, 4555 (1970).
[14]S. K. Ma and K. A. Brueckner, Phys. Rev. 165, 18 (1968).
[15]D. J. W. Geldart and M. Rasolt, Phys. Rev. B 13, 1477 (1976).
[16]D. J. W. Geldart and S. H. Vosko, Can. J. Phys. 44, 2137 (1966).
[17]For example, L. Hedin and S. Lundqvist, in *Solid State Physics*, edited by H. Ehrenreich, F. Seitz, and D. Turnbull (Academic, New York, 1969), Vol. 23.
[18]Note that integrating Eq. (49) by parts we could have avoided the need for the higher derivatives of $I_1(q)$ and $I_3(q)$ in Eq. (37) when calculating $\gamma_G(q)$. This, however, would not yield the more general result for $B_c(q)$ of Eq. (48).